Available online at www.sciencedirect.com

ScienceDirect

Procedia Engineering 109 (2015) 144 – 153

Procedia Engineering

www.elsevier.com/locate/procedia

XIII Italian Group of Fracture Meeting, IGFXXIII

Mechanical behaviour of a green sandwich made of flax reinforced polymer facings and cork core

Antonio Mancuso[a], Giuseppe Pitarresi[a]*, Davide Tumino[b]

[a] *Università degli Studi di Palermo, Dip. di Ingegneria Chimica, Gestionale, Informatica, Meccanica (DICGIM) - Palermo (Italy)*
[b] *Università degli Studi di Enna "Kore"- Facoltà di Ingegneria e Architettura – Enna (Italy)*

Abstract

This work investigates the flexural behavior of a composite sandwich made of flax fibers reinforced skin facings and an agglomerated cork core, to be employed as an eco-friendly solution for the making of structural components of small sailing boats. An experimental mechanical characterization of the strength and stiffness flexural behavior of the proposed sandwich is carried out, providing a comparison of performances from three implemented assembling techniques: hand-lay-up, vacuum bagging and resin infusion. Sandwich beams have been tested under three point bending (TPB) at various span lengths. A procedure is also proposed and implemented to consider the potential influence of the local elastic indentation in the experimental evaluation of the flexural stiffness. This procedure is based on the analytical solution of an indented beam resting on a fully backed Winkler foundation.

Peer-review under responsibility of the Gruppo Italiano Frattura (IGF)

Keywords: Composite Sandwich; Long Flax Fibres; Agglomerated Cork Core; Flexural Behaviour; Indentation; Winkler foundation.

1. Introduction

Fiber reinforced polymer composites represent a favorite candidate material in lightweight driven structural design. One driver of research in the last years has been the development of more eco-friendly composite concepts, either by obtaining raw materials from natural renewable sources, or by reducing the carbon footprint of raw materials production. Since a few years, these efforts have resulted in the advent of a number of commercial natural fibre reinforcements and natural core materials. Among natural fibers extracted from plants, Flax fibers are the leading choice when it comes to

* Corresponding author. Tel.: +39 091 23897281.
E-mail address: giuseppe.pitarresi@unipa.it

Peer-review under responsibility of the Gruppo Italiano Frattura (IGF)
doi:10.1016/j.proeng.2015.06.225

structural performances [1]. Their intrinsic stiffness is though still significantly smaller than traditional synthesized fiber reinforcements, e.g. glass and carbon. One well-known strategy to enhance the stiffness performances of a monolithic laminate is to assemble it in a sandwich structure, separating the laminate skin facings by an opportune core material [2]. In order to preserve the green footprint of the material, one interesting possibility is the combination of agglomerated cork panels as sandwich cores, with natural fibre reinforced face sheets [3,4]. The use of agglomerated cork as a sandwich core material, although only of recent development [5-8], has already demonstrated a number of advantages: good shear strength and stiffness [5,7], good thermal and acoustic insulation [7,9], good vibration damping [7,8], good damage tolerance to impact loads and general crashworthy performances [7,10], good drapability, good compatibility with thermoset resins and traditional composite manufacturing processes [6]. Furthermore, cork agglomerates with grain size, density, porosity and grain binders optimized for sandwich core applications are now commercially available [11].

The present work investigates the flexural stiffness and strength behavior of a sandwich made with commercial flax and cork raw materials. The sandwich skin faces are in particular made of a unidirectional flax fiber reinforced epoxy laminate, and the core material is a low-density agglomerated cork panel. The flexural behavior is investigated by means of variable span Three Point Bending (TPB) tests [12]. Flexural rigidity is obtained after decoupling the effects of shear. A procedure is also proposed to uncouple the potential influence of the local elastic indentation in the experimental evaluation of flexural and shear rigidity.

The experimental characterization is performed on three sandwich types, each differing for the manufacturing assembling technique: hand lay-up, vacuum bagging and resin infusion. It is found that each technique determines a significantly different amount of resin soaked into the cork core, which influences the mechanical behavior.

Finally it is noteworthy to report that the material studied in this work has been employed for the design and fabrication of two sailing dinghy hulls [13]. These boats have been designed and built at the University of Palermo (Italy) in order to participate in the inter-universities Italian regatta championships named “1001vela” [14]. The flax-reinforced-polymer/cork sandwich concept has been implemented and tested on the field, resulting in a successful primary hull structure concept.

2. Sandwich Concept

2.1. Materials

The fiber reinforcement used was Flaxdry UD-180-C003 supplied by *Lineo nv* (Belgium). This consisted of a 100% flax unidirectional fabric, with nominal areal weight of 180 g/m^2 (see also Fig. 1a). The epoxy resin used for lamination was SX-10 EVO (with a Medium hardener) for hand lay-up impregnation, and SX-8 EVO for resin infusion impregnation, both supplied by *Mates srl* (Italy). These resin systems achieved their fully cured condition after resting for 24 hours at room temperature, although the authors allowed more than one week time before cutting and testing samples. The core material consisted of a CoreCork NL10 panel supplied by *Amorim Cork Composites ACC* (Portugal), with nominal density of 140 kg/m^3 and nominal thickness of 6 mm.

2.2. Samples preparation

Three panels have been manufactured by three different processes: hand lay-up, hand lay-up plus vacuum bagging consolidation, and resin infusion. The three processes, and the relative samples, will hereinafter be referred by HL, VB and RI. Figure 1b shows a schematic of the manufacturing schemes, and Fig. 2 some pictures of different stages of production. A flat glass plate with a thin Mylar release film is used as base mould. Both the VB and RI processes have used a vacuum bag assembly, with an applied vacuum pressure higher than 0.95 bars. The areal dimensions of each panel were 500×350 mm^2, with the unidirectional flax fabric aligned along the short side. One side of the panel hosted the sandwich lay-up, with skin faces of $[0°]_3$ and a cork core laid in the middle, of dimensions 140×350 mm^2. The rest of the panel consisted of a monolithic $[0°]_6$ laminate. This allowed to obtain monolithic samples with a nominal fibre volume fraction and construction quality representative of the sandwich skin facings.

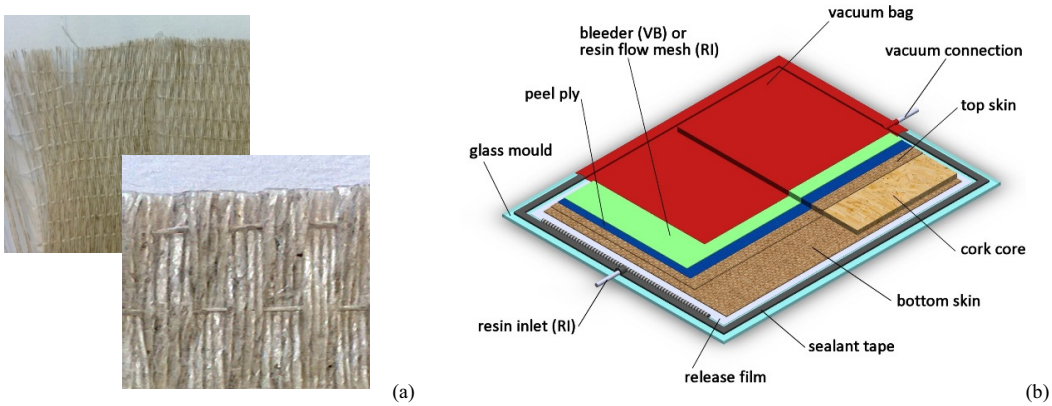

Fig. 1. (a) the UD flax fabric; (b) scheme of the VB and RI moulding.

Five sandwich beam samples of in-plane dimensions of 25×350 mm^2, and ten monolithic $[0°]_6$ samples of dimensions 15×250 mm^2 were cut form each of the three manufactured panels. Tensile samples were in particular prepared according to ASTM D3039, in order to measure the tensile Young's modulus representative of the sandwich skins. The thickness of the sandwich beams and of the monolithic $[0]_6$ panels ranged respectively between 7.7÷8.4 mm and 2÷2.4 mm, with the lowest values for the VB panel and the biggest for the HL panel.

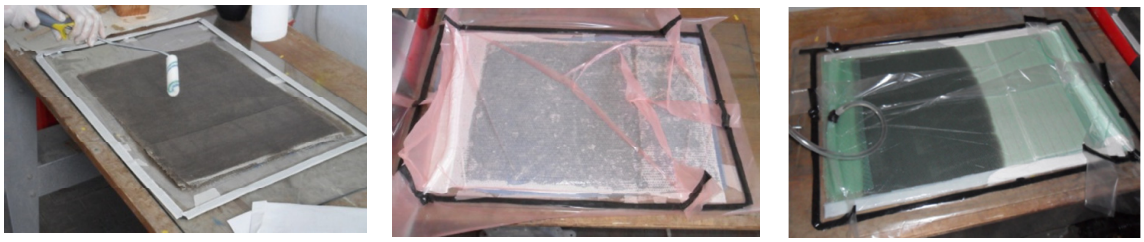

Fig. 2. (a) hand lay-up impregnation; (b) Vacuum bagging assembly; (c) intermediate stage of resin flowing in the resin infusion process.

All the cut monolithic samples from each panel were weighted in order to estimate the fibers volume fraction v_f. This was calculated by using the following formula, which neglects the void content:

$$v_f\,\% = \frac{V_c - V_m}{V_c} \times 100 = \frac{V_c - \left[\left(W_c - n \cdot A \cdot A_w\right)/\delta_m\right]}{V_c} \times 100 \tag{1}$$

where V, W and δ are volume, weight and density respectively, and the subscripts c, f, m refer to composite, fibre and matrix. A and A_w are the areal dimensions of the composite sample and the areal weight of the dry flax fabric, and n the number of layers. Table 1 summarises the calculated values of v_f. By knowing the nominal density of the cork core and of the laminate skins, it was possible, from weighting each single sandwich beam, to estimate also the amount of resin soaked into the cork core. This information is reported in table 1 as the percentage increase in weight of the cork core embedded into the sandwich.

Data summarized in table 1 indicate that the samples obtained from the three manufacturing processes differ significantly. In particular the VB is, as expected, able to provide the higher fiber volume fraction, being able to extract some excess resin into the bleeder layer. All three processes give rise to some resin soaking into the cork core, but with

significant differences. In particular, the RI process is the one able to better diffuse the resin within the core, bringing its final weight to a more than double value. It is noteworthy that also the HL process shows some degree of resin soaked by the core.

Table 1. Fractions of fibers and matrix in the laminates and core.

	HL	RI	VB
Fibers volume fraction, v_f [%]	39±1	42±1	50±3
% weight increase of cork core after sandwich manufacturing	33±10	122±7	65±5

3. Flexural behavior of sandwiches

The flexural and shear rigidity of beam sandwiches are usually obtained from three and/or four point bending tests (TPB and FPB), see e.g. ASTM C393 and ASTM D7250, based on first-order sandwich beam shear models [2,12,15]. By calling Δ the mid-span displacement, and adopting the same terminology of ASTM D7250, the general relation giving Δ as a function of the total applied load P is:

$$\Delta = \Delta_{flex} + \Delta_{shear} = \frac{P\left(2S^3 - 3SL^2 + L^3\right)}{96D} + \frac{P\left(S-L\right)}{4U} \tag{2}$$

Equation (2) comprises two terms, the first accounting for the flexural deflection is inversely proportional to the sandwich flexural rigidity D, and the second accounting for the shear deflection is inversely proportional to the sandwich shear rigidity U. The flexural mid-span deflection term is prominent with long spans, while shear deflection is usually not negligible for sandwiches, due to the low shear rigidity of core materials, and its relative contribution increases with reducing the support span S. In order to uncouple the flexural and shear effects, and determine experimentally D and U, more than one test is needed in TPB and/or FPB, where the support and load spans, S and L, are changed at each iteration.

In the present work, each sandwich sample has been tested five times in TPB, each time with a different S: 100, 150, 200, 250, 300 mm. Each test stopped before the onset of any permanent deformation or damage in the sandwich skin facings and core. The compliance slope from each test is obtained and, once it has been multiplied by the inverse of the correspondent support span, is plotted versus the square span length [12]. A linear regression of the obtained datasets is then the most convenient way to average the results and obtain D and U from the slope and intercept of the regression line, according to the following formula [12,15]:

$$\underbrace{\left(\frac{\Delta}{P}\right)\frac{1}{S}}_{y} = \underbrace{\frac{1}{48D}}_{m}\underbrace{S^2}_{x} + \underbrace{\frac{1}{4U}}_{q} \tag{3}$$

In the present work tensile tests on the monolithic samples and flatwise compression tests on square sandwich samples have provided experimental values of the sandwich skin and cork core Young's modules, E_{skin} and E_{core}, so that a direct evaluation of D can also be performed by [2]:

$$D = \frac{E_{skin}bt(d-t)^2}{2} + \frac{E_{skin}bt^3}{6} + \frac{E_{core}bc^3}{12} \tag{4}$$

3.1. Influence of flatwise indentation

The easiest way to measure the load *vs* mid-span displacement curve in a TPB set-up is by acquiring the signals of

the load cell and the crosshead displacement transducer of the testing machine. The crosshead displacement provides the measurement at the point of contact of the sample with the nose of the movable anvil at mid span. This measured displacement adds up to the flexural and shear deflections also a local indentation component. This indentation is in particular more relevant for skins with low flexural rigidity and cores with low compression stiffness.

One procedure to reduce this error is proposed here, based on the load *vs* indentation displacement solution, available in the literature for the easier case of a beam attached to a one-parameter elastic and fully backed Winkler foundation [16]. A scheme of the total mid span deflection and the three contributions of bending, shear and elastic indentation is shown in Fig. 3. By limiting the observation within the range of linear elastic behaviour of the core material and skin facing, the equation providing the indentation displacement is [17]:

$$P = 8D_{skin}\lambda^3\Delta_{ind} \tag{5}$$

where D_{skin} is the skin facing flexural rigidity:

$$D_{skin} = E_{skin} \cdot I_{skin} = \frac{E_{skin} \cdot bt^3}{12} \tag{6}$$

and λ is defined as:

$$\lambda = \sqrt[4]{\frac{E_{core} \cdot b}{c} \cdot \frac{1}{4D_{skin}}} \tag{7}$$

It is here observed that a more rigorous solution for the elastic indentation of a beam under TPB is provided by Steeves and Fleck [18]. It is though easy to verify that for the initial linear elastic range with low loads, the solution from [18] is very close and can be approximated to the prediction of the easier Eq. (5). One further advantage of Eq. (5) is that it can be easily combined with equation (4), giving:

$$\Delta = \Delta_{flex} + \Delta_{shear} + 1.5 \cdot \Delta_{ind} \quad \rightarrow \quad \underbrace{\left(\frac{\Delta}{P} - \frac{1.5}{8D_{skin}\lambda^3}\right)\frac{1}{S}}_{y} = \underbrace{\frac{1}{48D}}_{m}\underbrace{S^2}_{x} + \underbrace{\frac{1}{4U}}_{q} \tag{9}$$

where the constant elastic compliance term from Eq. 5, accounting for indentation, is subtracted to the experimentally measured global compliance term Δ/P. The indentation displacement is also incremented by a 1.5 factor to account for the indentation on the lateral support spans, which can be expressed by Eq. 5 but with a load that is half the value of the mid-span load.

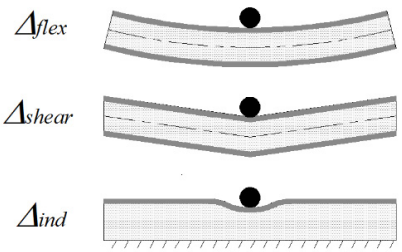

Fig. 3. Scheme of deflection components at the mid-span loading point of a TPB test.

4. Experimental results

Tensile tests on monolithic samples and flatwise compression tests on sandwich square samples have been carried out on a servo-hydraulic MTS 810 testing machine, equipped a with load cell of 100 kN. Deformation in tensile tests was measured by two HBM DD1 extensometers, resting on the two opposite side faces of the sample, with gauge length 25 mm. TPB sandwich beams have been carried out on an electro-mechanical Instron 3367 testing machine equipped with a 1 kN load cell.

4.1. Tensile behavior of sandwich skin faces

Figure 4a shows some typical stress *vs* strain curves measured on the three materials. All of them show a yield knee at around 30÷36 MPa, after which a significant change of slope occurs, although linearity is regained in the post-elastic zone. Such early yield knee is somewhat typical of flax yarns, as it has been observed by a few other authors for unidirectional flax thermoset laminates [19,20]. One explanation of this peculiar behaviour involves the influence of typical localised defects along flax fibres, usually referred to as "nodes" or "kink bands" [19]. These activate local fibre/matrix debonding phenomena at low stress levels, and behave as local more compliant portions of the fibre, which then tend to behave as if composed by a succession of linked short fibres. This eventually results in a macroscopic overall increase of compliance after onset of yielding [19,20].

Values of the longitudinal Young's modulus before the yield point, i.e. within the first linear elastic region, are given in table 2 for the three manufactured laminates.

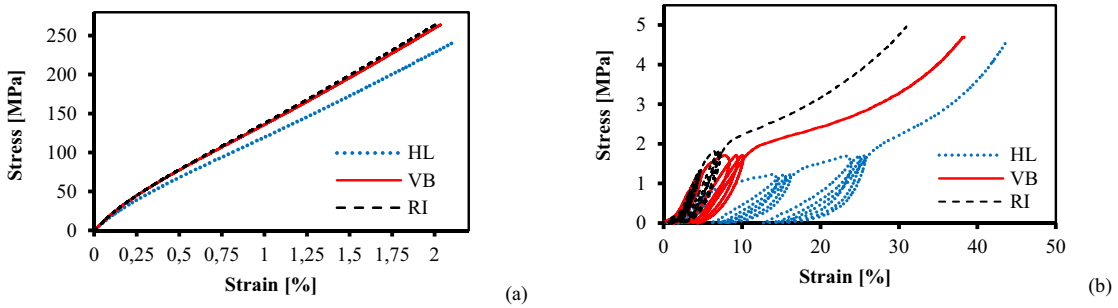

Fig. 4. (a) Tensile stress *vs* strain curves; (b) Flatwise compressive stress *vs* strain curves of sandwich samples.

4.2. Flatwise compression

Square 25×25 mm^2 sandwich samples were cut from the beam samples after flexural tests, and tested under flatwise compression. Care was taken in order to cut portions of the beam samples without any permanent damage or deformation from previous testing. Both monotonic and cyclic tests were performed. In particular the cyclic load history consisted in the successive application of three series of three loading-unloading cycles in load control, at the constant speed of 25 N/sec. The first series cycled between 0 and 500 N, the second between 0 and 800 N and the third between 0 and 1100 N. The measured nominal stress *vs* strain curves for the three sandwich types are shown in fig. 4b. Values of the Young's modulus in flatwise compression of the whole sandwich assembly, measured within the first linear elastic region, are given in table 2.

4.3. Flexural behavior: stiffness

Values of the sandwich flexural stiffness D, and shear stiffness U, obtained by the linear regression procedure of Eq. (3), and normalised by the sandwich beams width b (whose nominal value is 25 mm), are reported in table 2.

It is noteworthy to observe that the HL higher flexural stiffness is mainly due to the thicker skins determined by a lower fibre volume fraction, being the lay-up the same in all panels. The increment of thickness in the sandwich, due

to a lower fibre volume fraction, has a predominant effect on D, with respect to increments in the skins and core Young's modules.

Some more marked differences between the three sandwiches are observed regarding their shear rigidity U. In this case the trend for U seems to correlate well the amount of resin soaked by the core (see table 1). The RI panel has the highest shear rigidity, more than twice the HL, and the highest increase in cork core weight.

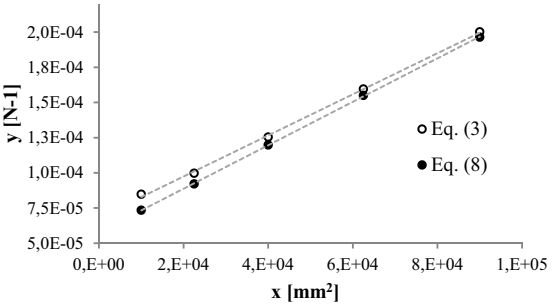

Fig. 5. Linear regression points of Eqs. 3 and 8 for an HL sandwich.

Table 2. Measured values of stiffness for skins, core and sandwich beams.

	HL	RI	VB
E_{skin} [GPa]	17.7±0.55	20.4±0.49	22±0.67
E_{core} [MPa]	16.6	34.2	30.7
D/b [N·m]	580±13	517±10	473±12
U/b [N/mm]	153±7	350±26	250±19

The procedure outlined in section 3.1, aimed at considering the potential influence of indentation on the stiffness characterization, has been found to provide some meaningful results for the HL sandwich. In fact the HL is more prone to develop early indentation due to the significantly lower core compression stiffness. Results from comparing the two linear regression procedures, the classic one of Eq. (3) and the new one of Eq. (8), are summarized in Table 3. Here two HL beam samples have been analyzed. Each sample is tested twice, with the second test performed with the sample flipped upside down. Since the sandwich is nominally symmetric, the theoretical value of D from Eq. (4) does not depend on the faces position in the testing rig.

Table 3. HL beam sandwich: comparison of results.

	beam 1	beam 1 flipped	beam 2	beam 2 flipped	Avg ± st.dev
Correlation coefficient R^2 (Eq. 3)	0.9994	0.9966	0.9991	0.9968	
Correlation coefficient R^2 (Eq. 8)	0.9994	0.9997	0.9999	0.9989	
D/b (Eq. 4) [N·m]	542.2	542.2	533.1	533.1	537.6±5
D/b (Eq. 3) [N·m]	587.7	594.8	570.2	568.7	580.3±13
D/b (Eq. 8) [N·m]	544.2	550.3	539.0	528.0	540.4±9
U/b (Eq. 3) [N/mm]	149.6	153.6	146.1	146.3	148.9±4
U/b (Eq. 8) [N/mm]	188.9	194.6	172.2	183.6	184.8±10

Figure 5 shows an example of the linear regression points of Eq. (3) and Eq. (8) for an HL sample. It is observed in particular that the line interpolating the points of Eq. (8) is steeper. This behavior is found in all the analyzed datasets, and is determined by the fact that the correction for the indentation term is bigger at low spans. A consequence is that the linear regression procedure of Eq. (8) provides a smaller value of flexural stiffness D and a higher value of shear stiffness U compared to neglecting the indentation correction, i.e. using Eq. (3). Results in table 3 show that the correlation coefficient R^2 is very good for both linear regressions, yet slightly higher for Eq. (8). A more significant outcome is that the values of D predicted by Eq. (8) are much closer to the values from Eq. (4), than those found with Eq. (3). Another interesting result is that the shear rigidity U seems to change more than D, in relative terms, when using the modified linear regression of Eq. (8). A potential conclusion is then that the local indentation has a more marked influence on the evaluation of the shear rigidity, which is higher than that evaluated by not taking into account indentation at the loading points.

4.4. Flexural behavior: strength

The failure behaviour in TPB was investigated with span 100 mm, and hence a nominal value of $S/d \approx 100/8 = 12.5$, and with S=250 mm ($S/d \approx 31$)). The load *vs* mid-span displacement curves for the two spans are shown in Fig. 6. It is observed that each sandwich type is reported twice, with the second sample tested by changing the skin face in compression. The RI and VB samples in particular evidenced some differences in terms of failure load, depending of which face is loaded in compression. It was observed in particular that the higher loads are obtained when the compressed face is the one that rested against the mould during the sandwich manufacturing. Although it was difficult to take a precise measure of the thickness of the two skins, it is believed that the skin resting against the mould might have developed a slightly higher thickness, due to a higher amount of resin extraction occurring on the side of the vacuum bag. The maximum failure load for both span values occurred at the onset of indentation of the loading nose onto the cork core. Hence, when the upper face is the thicker skin, indention requires a higher load to onset. Figure 7 reports some pictures of the failure accumulation at high mid-span displacements.

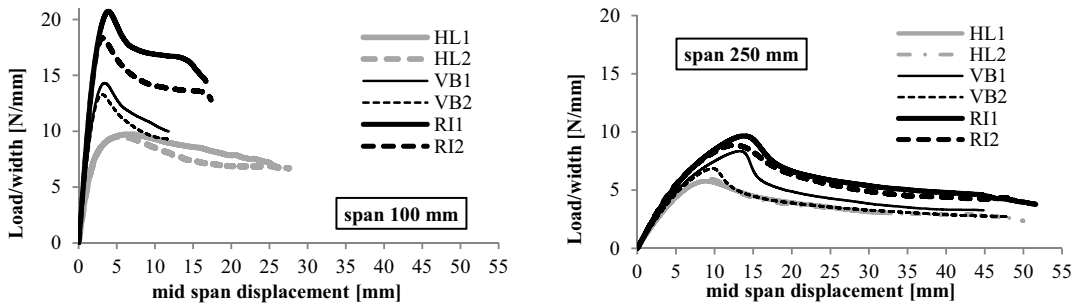

Fig. 6. Three Point Bending load *vs* mid-span displacement curves for S=100 mm (left) and S=250 mm (right).

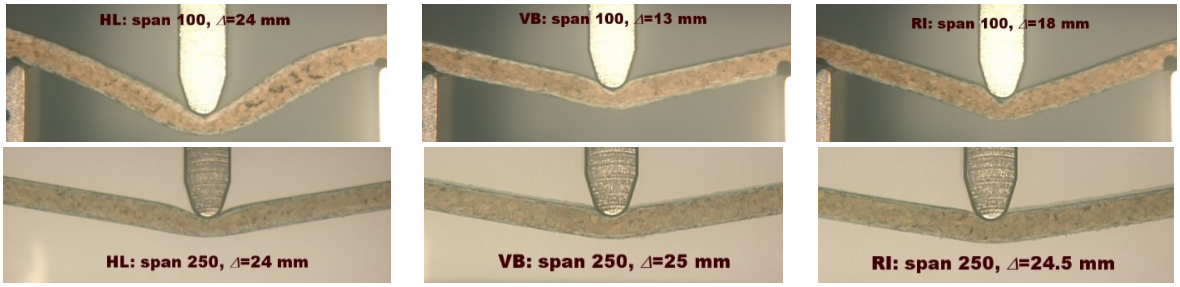

Fig. 7. Pictures of failing sandwich beams under Three Point Bending 100 mm and 250 mm span lengths.

In general, it was observed that failure onset was always by the indentation of the loading nose. Only for HL samples and span of 100 mm it was possible to reach a final shear failure of the core (see in Fig. 7), while in all other cases the indention of the loading nose went on until eventually reaching compression failure of the skin, after which the failed mid-span zone behaved similarly to a plastic hinge.

Table 4 reports values of the membrane skin stress and mid-span shear stress, calculated according to the formulas provided by ASTM C393 [7]:

$$\sigma_{max} = \frac{P_{max} L}{2t(d+c)b}; \quad \tau_{max} = \frac{P_{max}}{(d+c)b}; \tag{9}$$

The reported values in Table 4 are in particular calculated at the maximum load reached during the TPB test.

Regardless of the non-symmetrical behaviour commented before, it is noteworthy how the RI sandwich reached the higher failure stresses, while the HL sandwich has the lower values. The ability of the RI to resist more to the onset of indentation is probably correlated with the higher amount of resin soaked into the core, which makes this sandwich beam about twice more resistant than HL.

It is finally evidenced how the maximum stresses σ_{max} in Table 4 are usually higher than 30 MPa, which was indicated as the yield point in the tensile tests on unidirectional flax reinforced monolithic laminates (see Fig. 4a). The TPB curves became non-linear with increasing load, but do not evidence a sudden change of slope. It is though likely that the onset of non-linear behaviour is somewhat favoured by the non-linear transition between the first elastic and the second post-elastic linear segments observed in the tensile curves of monolithic samples.

Table 4. Average values of σ_{max} and τ_{max} (defined by Eq. 9) at maximum load [MPa].

	Span [mm]	HL	thicker skin compressed		thinner skin compressed	
			RI	VB	RI	VB
σ_{max}	100	29.0	69.9	56.0	60.4	52.9
τ_{max}	100	0.72	1.47	1.25	1.27	1.04
σ_{max}	250	49.5	84.2	80.4	77.4	66.2
τ_{max}	250	0.42	0.71	0.63	0.65	0.52

5. Conclusions

In this work a green sandwich concept has been considered, employing an agglomerated cork core and unidirectional Flax reinforced epoxy skin facings. All the constituent materials used are available in the market. Both monolithic and sandwich panels have been manufactured by implementing three different techniques: Hand Lay-up (HL), Vacuum Bagging (VB) and Resin Infusion (RI). The three techniques have been found to provide some differences in the tensile behavior of the monolithic laminates and the flexural behavior of beam sandwiches. In particular these differences arise due to the different fiber volume fractions (higher for VB), and different amounts of resin soaked into the cork core (higher for RI). This last in particular, although giving a weight penalty due to the higher density of the final sandwich, has been found to be highly beneficial in terms of shear rigidity and flexural strength.

The work has also confirmed the presence of a bilinear tensile behavior of the unidirectional flax reinforced laminate, with the onset of an early yield point probably induced by the typical “kink band” defects present in flax fibers. This early yield stress has not influenced the stiffness characterization of the sandwich, due to the low loads needed for this elastic characterization. An influence is instead likely to occur in the marked non-linear behavior observed in the sandwich Three Point Bending curves near the onset of failure.

The present work also has proposed a procedure to evaluate the flexural behavior of sandwich beams that is able to decouple the influence of bending, shear and local indentation at the loading points. Regarding indentation, this is obtained by considering the linear elastic relationship between load and displacement in a facing attached to a one-parameter Winkler type fully backed foundation. This relationship is in particular integrated into the general load *vs* mid-span displacement relationship of a Three Point Bending set-up, and decoupling is finally achieved by performing tests at different span lengths. The novel procedure has been implemented with some interesting outcomes in the case of the HL sandwich beams, indicating that neglecting local indentation might results in a significant underestimation of the shear rigidity and an overestimation of the flexural rigidity.

Acknowledgements

The authors would like to thank Mr. Francesco Carabellò and Mr. Salvatore Valenti for their help during the preparation and testing of samples, the rector of the University of Palermo, Prof. Roberto Lagalla, for supporting the activities of the Zyz Saling team (see Fig. 8), and the company Amorim Cork Composites ACC (Portugal) for kindly supplying the cork material tested in this work.

Fig. 8. *LED (Linen Epoxy Dinghy)*, one of the Zyz sailing team's dinghies implementing the sandwich concept presented in this work. On the right, *LED* during the regatta in Tuscany (IT) in 2010 (helmsman: Mr. Alessio Frazzitta; forward: Mr. Mauro Utzeri) [14].

References

[1] L. Yan, N. Chouw, K. Jayaraman. Flax fibre and its composites - A review. Compos Part B: Eng. 56 (2014) 296-317.
[2] L.A. Carlsson, G.A. Kardomateas, Structural and Failure Mechanics of Sandwich Composites, In series: Solid Mechanics and its Applications 121, Springer Science. 2011.
[3] R. Hoto, G. Furundarena, J.P. Torres, E. Muñoz, L. Andrés, J.A. García. Flexural behavior and water absorption of asymmetrical sandwich composites from natural fibers and cork agglomerate core. Mater Lett. 127 (2014) 48-52.
[4] N. Lakreb, B. Bezzazi, H. Pereira. Mechanical behavior of multilayered sandwich panels of wood veneer and a core of cork agglomerates. Materials and Design. 65 (2015) 627-36.
[5] L. Reis, A. Silva. Mechanical behavior of sandwich structures using natural cork agglomerates as core materials. Journal of Sandwich Structures and Materials. 11(6) (2009) 487-500.
[6] L. Gil. Cork composites: A review. Materials. 2(3) (2009) 776-89.
[7] O. Castro, J.M. Silva, T. Devezas, A. Silva, L. Gil. Cork agglomerates as an ideal core material in lightweight structures. Materials and Design. 31(1) (2010) 425-32.
[8] R.A.S. Moreira, F.J.Q. De Melo, J.F. Dias Rodrigues. Static and dynamic characterization of composition cork for sandwich beam cores. J Mater Sci. 45(12) (2010) 3350-66.
[9] J. Sargianis, H. Kim, J. Suhr. Natural cork agglomerate employed as an environmentally friendly solution for quiet sandwich composites. Scientific Reports 2 (2012).
[10] J. Sousa-Martins, D. Kakogiannis, F. Coghe, B. Reymen, F. Teixeira-Dias. Behaviour of sandwich structures with cork compound cores subjected to blast waves. Eng Struct. 46 (2013) 140-146.
[11] http://www.amorimcorkcomposites.com/ .
[12] H.G. Allen, Analysis and Design of Structural Sandwich Panels, Pergamon Press, Oxford, 1969.
[13] T. Ingrassia, A. Mancuso, V. Nigrelli, D. Tumino. A multi-technique simultaneous approach for the design of a sailing yacht. Int J Interact Des Manuf. (2015) DOI 10.1007/s12008-015-0267-2.
[14] http://www.dicgim.unipa.it/zyz/.
[15] D. Tumino, T. Ingrassia, V. Nigrelli, G. Pitarresi, V. Urso Miano. Mechanical behavior of a sandwich with corrugated GRP core: numerical modeling and experimental validation. Frattura ed Integrità Strutturale. 30 (2014) 317-326.
[16] G. Pitarresi, J. Amorim. Indentation of rigidly supported sandwich beams with foam cores exhibiting non-linear compressive behaviour. Journal of Sandwich Structures and Materials. 13(5) (2011) 605-36.
[17] D. Zenkert, A. Shipsha, K. Persson. Static indentation and unloading response of sandwich beams. Compos Part B. 35 (2004) 511–522.
[18] C.A. Steeves, N.A. Fleck. Collapse mechanisms of sandwich beams with composite faces and a foam core, loaded in three-point bending. Part I: Analytical models and minimum weight design. Int J Mech Sci. 46(4) (2004) 561-583.
[19] M. Hughes, J. Carpenter, C. Hill. Deformation and fracture behaviour of flax fibre reinforced thermosetting polymer matrix composites. J Mater Sci. 42(7) (2007) 2499-2511.
[20] R.H. Newman, M.A. Battley, J.E.P. Carpenter, M.J. Le Guen. Energy loss in a unidirectional flax-polyester composite subjected to multiple tensile load-unload cycles. J Mater Sci. 47(3) (2012) 1164-1170.